

# Role of Cationic Organisation on Water Dynamics in Saponite Clays

Virginie Marry,<sup>\*,†</sup> Sébastien Le Crom,<sup>†</sup> Eric Ferrage,<sup>‡</sup> Laurent Michot,<sup>†</sup> Bela  
Farago,<sup>¶</sup> Alfred Delville,<sup>§</sup> and Emmanuelle Dubois<sup>†</sup>

<sup>†</sup>*Sorbonne University, Laboratoire PHENIX UMR CNRS 8234, 4 place Jussieu, case 51,  
75005 Paris, France*

<sup>‡</sup>*IC2MP-Hydrasa, UMR 7285, CNRS, Université de Poitiers, 5 rue Albert Turpain, Bât.  
B8, TSA 51106, 86073 Poitiers cedex 9, France*

<sup>¶</sup>*Institut Max von Laue-Paul Langevin (ILL), 71 Avenue des Martyrs, CS 20156, F-38042  
Grenoble Cedex 9, France*

<sup>§</sup>*ICMN, UMR 7374, CNRS-Université d'Orléans, 1b rue de la Férollerie, CS 40059, 45071  
Orléans cedex, France*

E-mail: virginie.marry@sorbonne-universite.fr

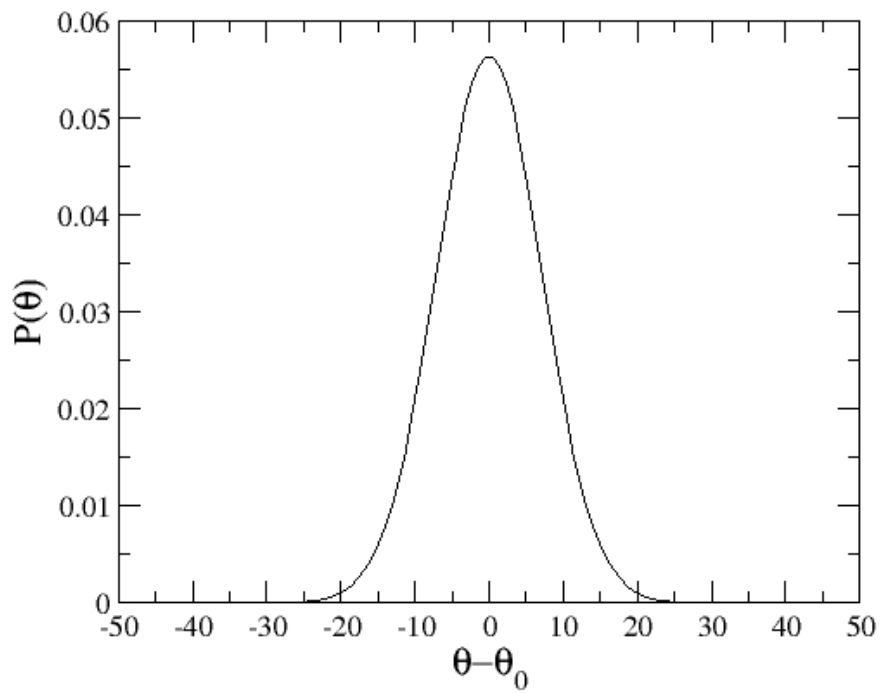


Figure S1: Probability to find a clay layer with an orientation  $\theta$  around  $\theta_0$  with  $\Delta\theta=10^\circ$ .

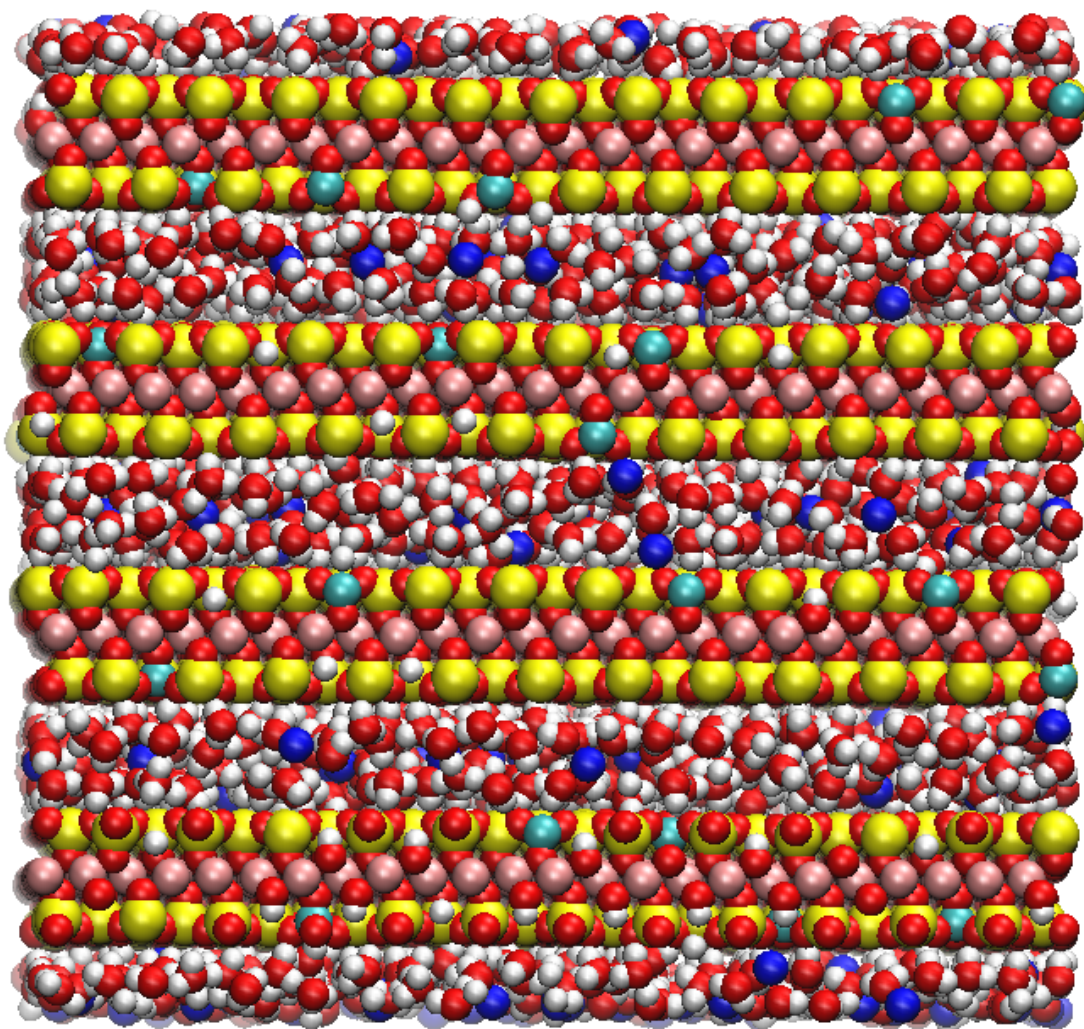


Figure S2: Example of snapshot obtained from molecular dynamics simulations. Red: Oxygen atoms; white: Hydrogen; Dark blue:  $\text{Na}^+$ ; Yellow: Si; Pink: Mg; Light Blue: Al

---

## Elements for demonstrating the expression of $S_{mod}(\mathbf{Q},t)$

Considering a motion in three-dimensions bound only in the direction  $z$ , the expression  $S(\mathbf{Q},\omega)$  derived by Bee et al<sup>1</sup> can be written as  $S_{z-bounded}(\mathbf{Q},t)$ :

$$S_{z-bounded}(\mathbf{Q},t) = e^{-D_{\parallel}(Q_x^2+Q_y^2)t} \int_{-L}^L p(z,t) \cos(Q_z z) dz \quad (\text{S1})$$

where  $L$  is the distance of confinement and  $p(z,t)$  is the probability to find an H atom at time  $t$  at the position  $z$ , given that it was at the origin at  $t = 0$ .  $Q_x$ ,  $Q_y$  and  $Q_z$  are the coordinates of the wavevector  $\mathbf{Q}$ . If the density of H atoms in the interlayer is assumed to be uniform, the diffusion equation verified by  $p(z,t|z_0,0)$ , the probability to find the atom at  $(z,t)$  when at  $z_0$  at  $t = 0$ , is

$$\frac{\partial p(z,t|z_0,0)}{\partial t} = D_{\perp} \frac{\partial^2 p(z,t|z_0,0)}{\partial z^2} \quad (\text{S2})$$

where  $D_{\perp}$  is the diffusion coefficient perpendicular to the clay layers. With reflecting boundary conditions on the walls, the above equation has an analytical solution which can be written in the form of a series expansion<sup>1</sup> :

$$p(z,t|z_0,0) = \frac{1}{L} + \frac{2}{L} \sum_{n=1}^{\infty} \cos\left(\frac{n\pi z}{L}\right) \cos\left(\frac{n\pi z_0}{L}\right) e^{-\frac{n^2\pi^2 D_{\perp} t}{L^2}} \quad (\text{S3})$$

Assuming  $z' = z - z_0$ ,  $p(z,t|z_0,0)$  can be integrated over all possible values of  $z_0$ , i.e. between 0 and  $L - z'$  for  $z' > 0$ <sup>1</sup> :

$$p(z',t) = \frac{L - z'}{L^2} + \sum_{n=1}^{\infty} \left[ \frac{L - z'}{L^2} \cos\left(\frac{n\pi z'}{L}\right) - \frac{1}{nL\pi} \sin\left(\frac{n\pi z'}{L}\right) \right] e^{-\frac{n^2\pi^2 D_{\perp} t}{L^2}} \quad (\text{S4})$$

which leads to :

$$\begin{aligned} \int_0^L p(z', t) \cos(Q_z z') dz' &= \frac{(1 - \cos(Q_z L))}{Q_z^2 L^2} \\ &+ \sum_{n=1}^{\infty} (1 - (-1)^n \cos(Q_z L)) \frac{2Q_z^2 L^2}{(n^2 \pi^2 - Q_z^2 L^2)^2} e^{\frac{-n^2 \pi^2 D_{\perp} t}{L^2}} \end{aligned} \quad (S5)$$

Using similar reasoning for  $z' < 0$ , after integrating  $z_0$  between  $-z'$  and  $L$ , we finally obtain :

$$\begin{aligned} \int_{-L}^L p(z', t) \cos(Q_z z') dz' &= \frac{2(1 - \cos(Q_z L))}{Q_z^2 L^2} \\ &+ 2 \sum_{n=1}^{\infty} (1 - (-1)^n \cos(Q_z L)) \frac{2Q_z^2 L^2}{(n^2 \pi^2 - Q_z^2 L^2)^2} e^{\frac{-n^2 \pi^2 D_{\perp} t}{L^2}} \end{aligned} \quad (S6)$$

In order to take into account the mosaicity, we must average this result over  $\theta$ , the angle between the wave-vector  $\mathbf{Q}$  and the direction perpendicular to the clay layers.

Considering a distribution of orientations  $P(\theta)$ , such that  $\int_0^{\pi} P(\theta) d\theta = 1$ , we get :

$$S^{mod}(Q, t) = \langle S_{z-bounded}(Q, t) \rangle_{\theta} = \int_0^{\pi} P(\theta) e^{-D_{\parallel}(Q_x^2 + Q_y^2)t} \int_{-L}^L p(z, t) \cos(Q_z z) dz d\theta \quad (S7)$$

With  $Q_z = Q \cos \theta$  and  $Q_x^2 + Q_y^2 = Q^2(1 - \cos^2 \theta)$ , we arrive at :

$$\begin{aligned} S^{mod}(Q, t) &= 2e^{-D_{\parallel} Q^2 t} \left[ \int_0^{\pi} d\theta P(\theta) e^{D_{\parallel} Q^2 \cos^2 \theta t} \left( \frac{1 - \cos(Q L \cos \theta)}{Q^2 L^2 \cos^2 \theta} \right) \right. \\ &\left. + \sum_{n=1}^{\infty} 2e^{\frac{-n^2 \pi^2 D_{\perp} t}{L^2}} \int_0^{\pi} d\theta P(\theta) e^{D_{\parallel} Q^2 \cos^2 \theta t} \left( \frac{Q^2 L^2 \cos^2 \theta (1 - (-1)^n \cos(Q L \cos \theta))}{(n^2 \pi^2 - Q^2 L^2 \cos^2 \theta)^2} \right) \right] \end{aligned} \quad (S8)$$

Here  $P(\theta)$  was modeled by a gaussian centered on  $\theta_0$ ,  $P(\theta) = P_0 \exp -\frac{(\theta - \theta_0)^2}{\Delta \theta^2}$ . Numerically, the integral over  $\theta$  was calculated between  $\theta_0 - 5\Delta\theta$  and  $\theta_0 + 5\Delta\theta$ , the function being negligible beyond.

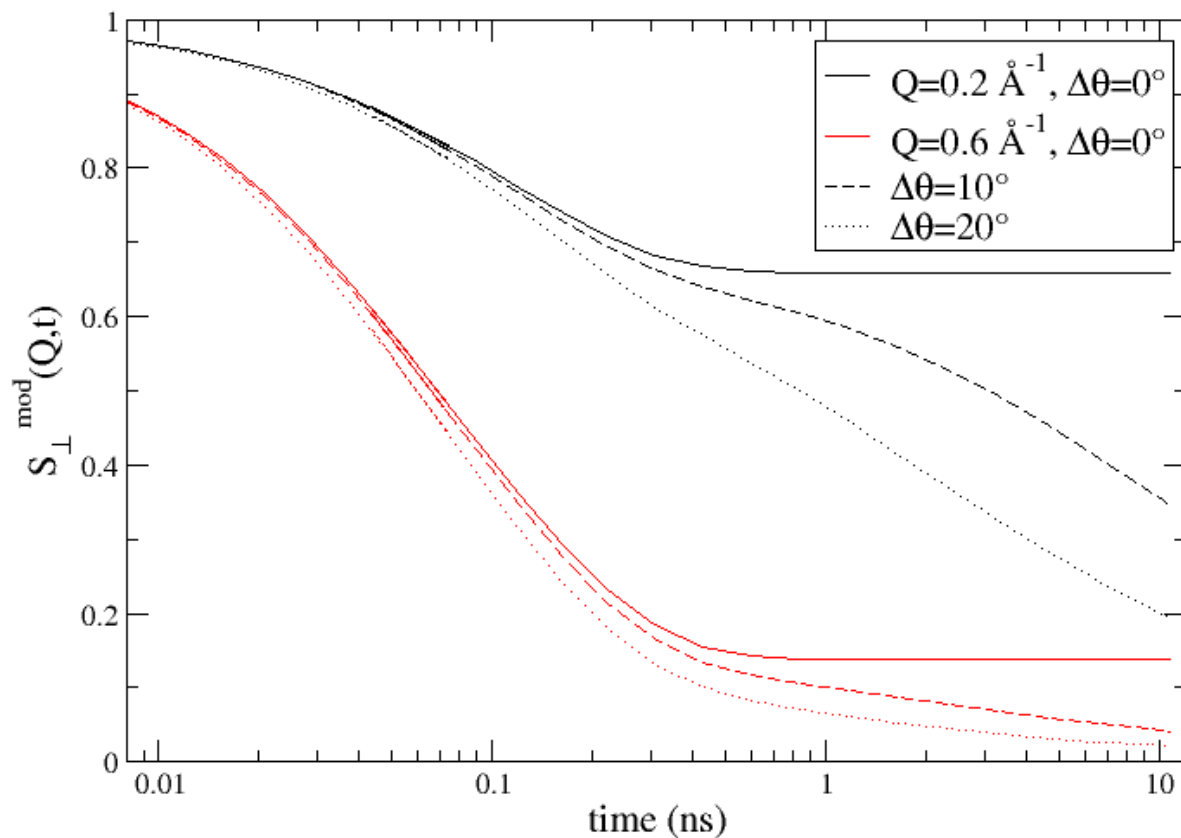


Figure S3:  $S_{\perp}(Q, t)$  obtained with the model of equation 7, with  $D_{\parallel} = 8.9 \times 10^{-10} \text{ m}^2 \cdot \text{s}^{-1}$  and  $D_{\perp}/D_{\parallel}=0.5$ . Black:  $Q=0.2 \text{ \AA}^{-1}$ , red:  $Q=0.6 \text{ \AA}^{-1}$ . Solid line: pure perpendicular diffusion ( $\Delta\theta = 0$ ), dashed line:  $\Delta\theta = 10^\circ$ , dotted line:  $\Delta\theta = 20^\circ$ . In the case of pure perpendicular diffusion,  $S_{\perp}(Q, t)$  decreases towards a plateau which is higher at lower  $Q$ s. The mosaicity causes the decrease of  $S_{\perp}(Q, t)$  down to 0 (note that immobile hydrogens are not taken into account in this calculation). This decrease is all the more rapid as the mosaicity and  $D_{\parallel}$  are high.

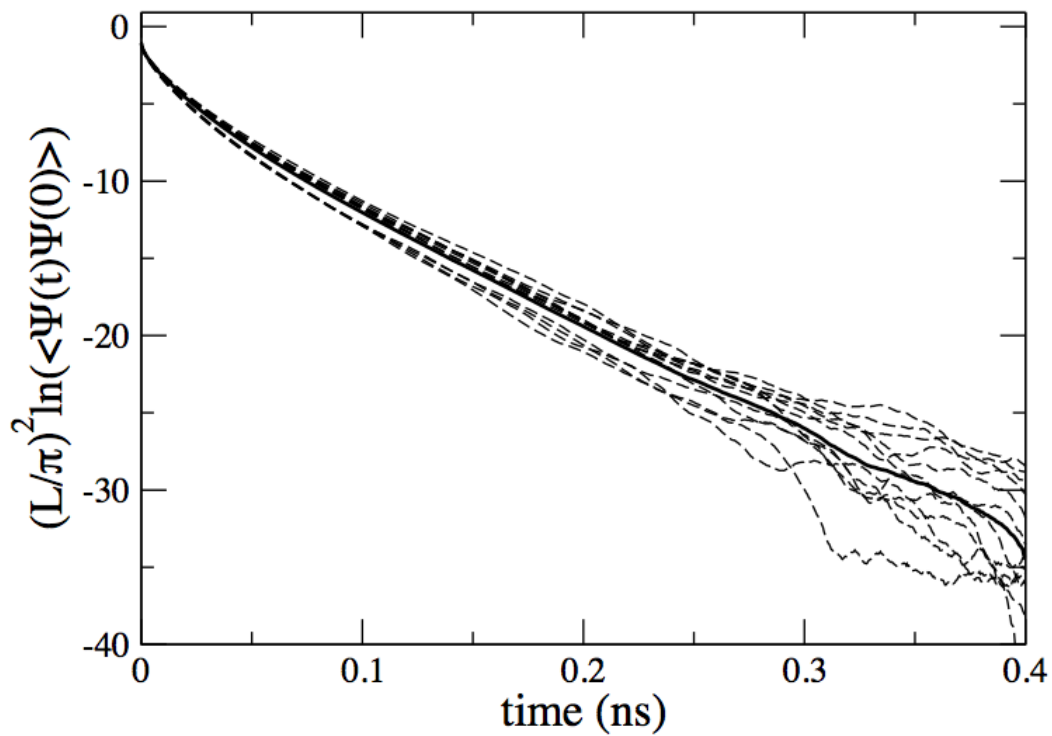


Figure S4: Auto-correlation function of  $\Psi(t)$  for TIP4P2005/clayFF at  $T=300$  K. The thick black line is the average of the other curves, which corresponds to the different interlayers spaces analyzed.

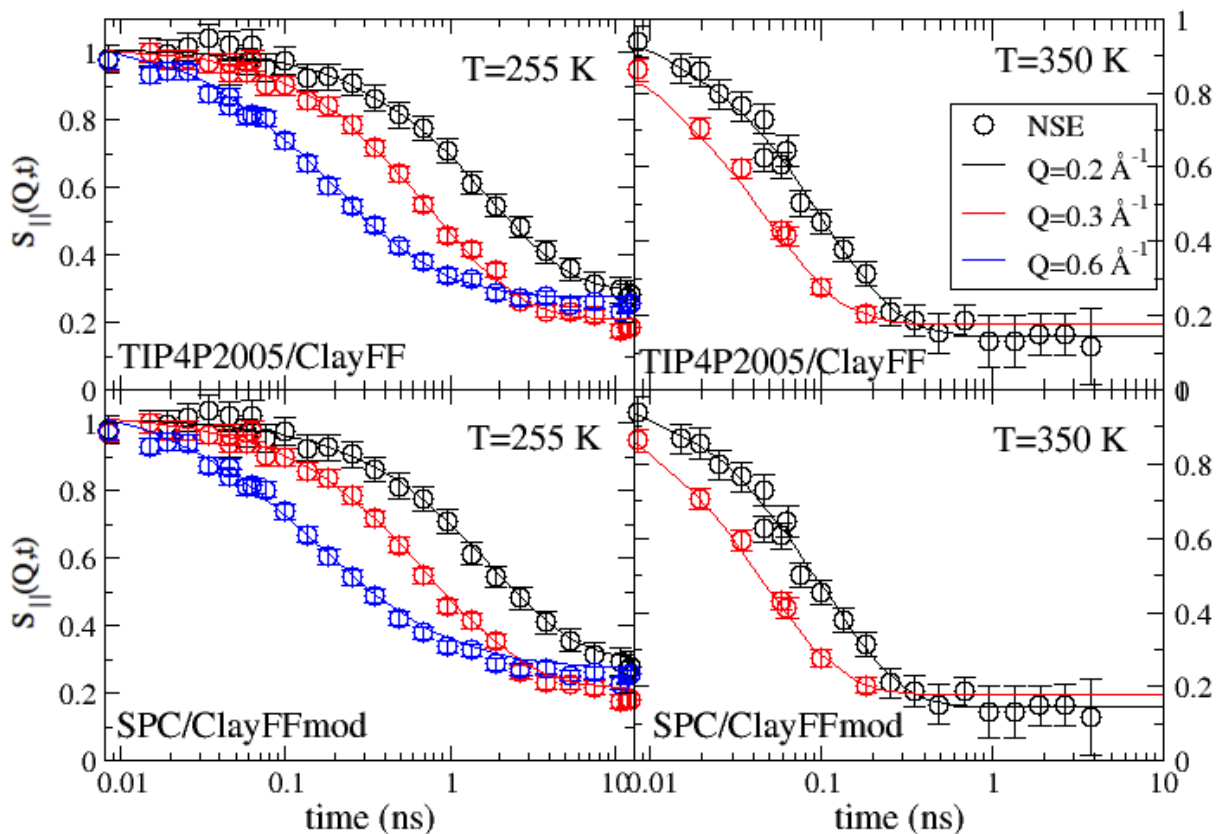


Figure S5: Comparison of experimental and transformed simulated  $S_{||}(Q, t)$  at T=255K (left) and T=350K (right) with TIP4P2005/clayFF (top) and SPC/ClayFFmod (bottom). Relaxation times (abscissa) have been multiplied by a factor in order to fit the experimental data at best. Black:  $Q = 0.2 \text{ \AA}^{-1}$ , red:  $Q = 0.3 \text{ \AA}^{-1}$ , blue:  $Q = 0.6 \text{ \AA}^{-1}$ . Solid line: simulations, circles: NSE experiments.



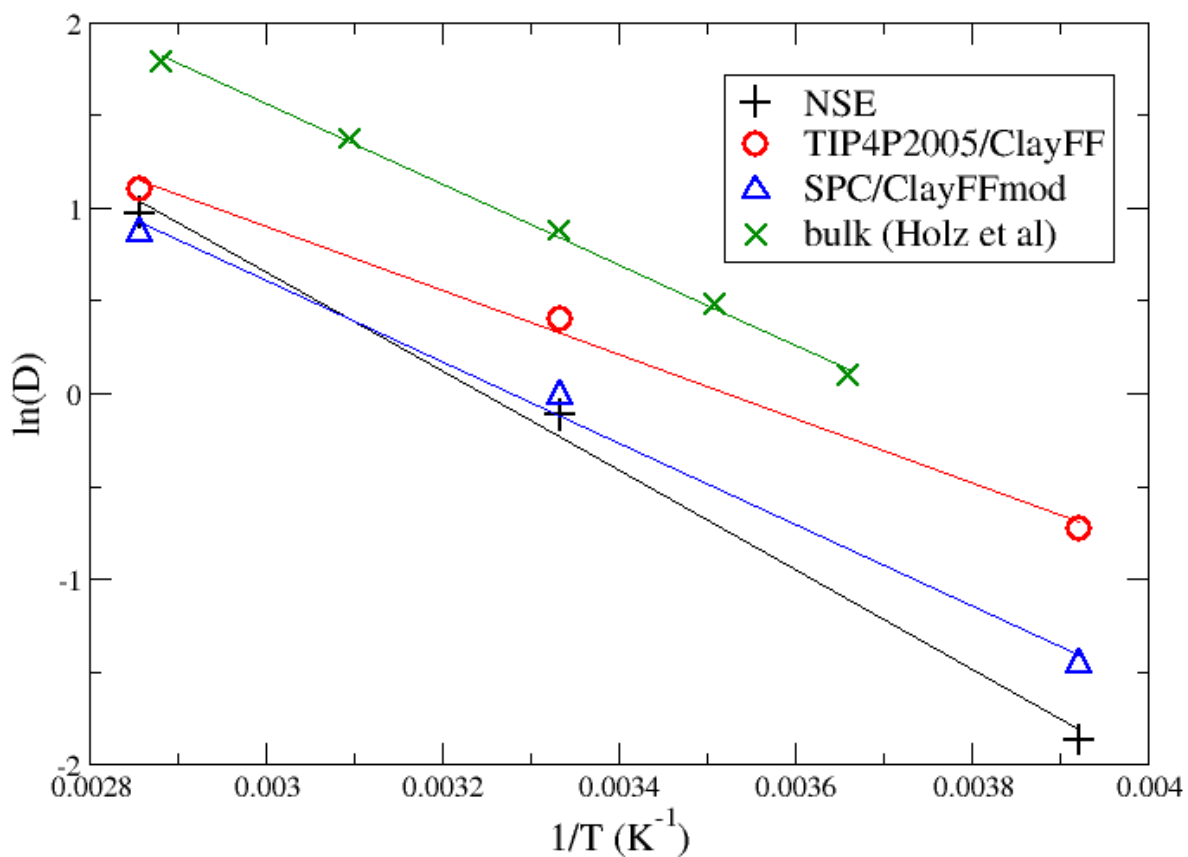


Figure S6:  $\ln(D)$  as a function of  $1/T$  for water in bihydrated saponite from NSE experiments and simulations (black plus: NSE experiment, red circles: TIP4P2005/ClayFF, blue triangles: SPC/ClayFFmod) and bulk water from NMR experiments (green crosses). Linear regressions are indicated by solid lines.

---

# Methodology for the calculation of MSD of water molecules inside and outside cation hydration spheres.

From radial distribution functions  $g_{\text{NaOW}}$  between sodium ions and water oxygens (see figure S8), the first minimum  $R_{\text{min}}$  at 3.2 Å can be taken as the radius of the hydration sphere. Then a water molecule is considered inside the hydration sphere when its distance to a cation is less than  $R_{\text{min}}$  (state 0) and outside when it is higher than  $R_{\text{min}}$  (state 1). In order to calculate the MSD of molecules inside hydration spheres, only molecules in state 0 must be counted. Thus, a molecule in state 0 initially must be discarded in the MSD calculation as soon as it leaves the hydration sphere. However, some of the molecules located at a distance close to  $R_{\text{min}}$  from the cations make some unsuccessful attempts to leave the hydration sphere by going shortly to state 1 and return rapidly to state 0, because of relatively low energy barriers between the two states. If  $R_{\text{min}}$  is taken as a strict limit between state 0 and state 1, these molecules are rapidly lost for the calculation of residence time and mean-squared displacement, although it would be more physical to consider that they remain in state 0. Moreover, these molecules are even faster lost when the time step between two configurations decreases, which makes the results dependent on the time step. That is why we chose a different definition of states 0 and 1.

Approximating the mean force potential between  $\text{Na}^+$  and OW as  $k_B T \ln(g(r))$  and following the SSP (stable state picture) approach described in ref,<sup>2</sup> a molecule is considered in state 0 if its distance to the cation is lower than the position of half the energy barrier necessary to go from state 0 to state 1. Likewise, a molecule is considered in state 1 if its distance to the cation is higher than the position of half the energy barrier necessary to go from state 1 to state 0. These two distances are 2.7 and 3.7 Å respectively and are indicated by pluses on figure S8. Then a molecule initially in state 0 is considered to remain in state 0 as long as its distance to the cation remains less than 3.7 Å. Likewise, a molecule initially in state 1 is considered to remain in state 1 as long as its distance to the cation remains

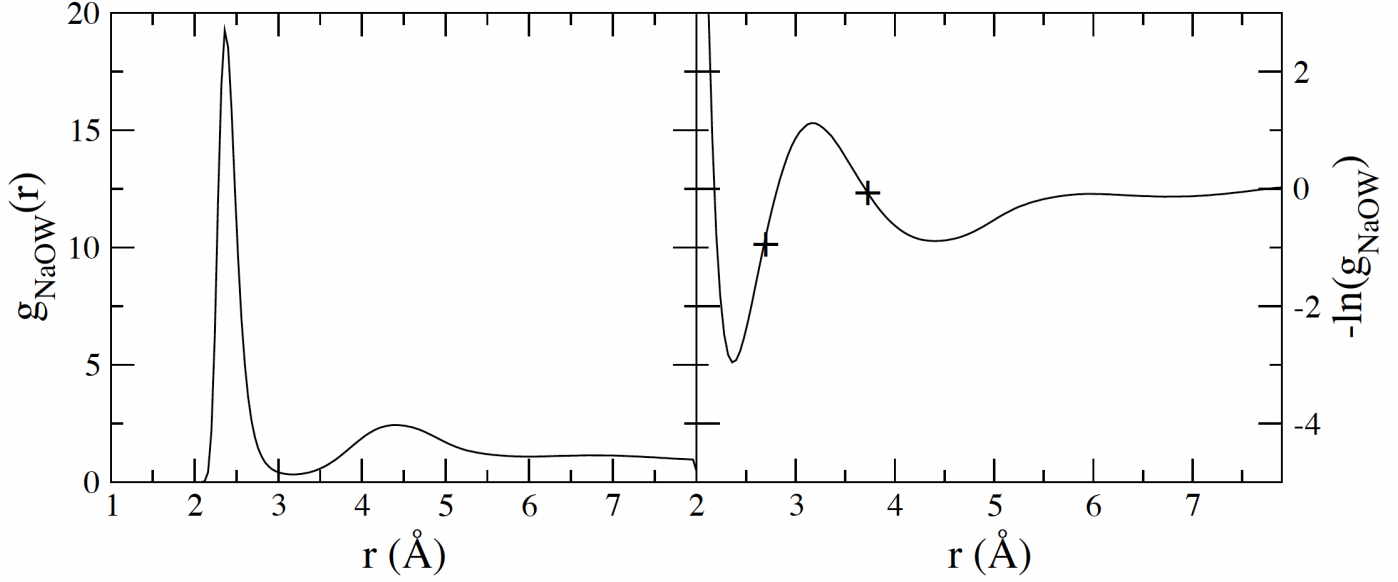


Figure S7: Left:  $g_{\text{NaOW}}(r)$  in bihydrated saponite with SPC/clayFFmod force field. Right: approximated mean force potential between  $\text{Na}^+$  and OW ( $k_B T$  units).

more than 2.7 Å. It allows to discard fast recrossings between the two states and to strongly attenuate the time step dependence.

The mean-squared displacement of molecules in state  $i$  is then calculated using:

$$MSD^i(t) = \frac{\langle (\Delta x^2(t) + \Delta y^2(t)) S^i(t) \rangle}{\langle S^i(t) \rangle} \quad (\text{S9})$$

where  $S^i(t)=1$  if the molecule remains continuously in state  $i$  between 0 and  $t$  in the frame of the SSP approach, and  $S^i(t)=0$  otherwise. The angle brackets denote the average over the molecules.  $\langle S^i(t) \rangle$  can also be approximated by a decreasing monoexponential in order to deduce a residence time.

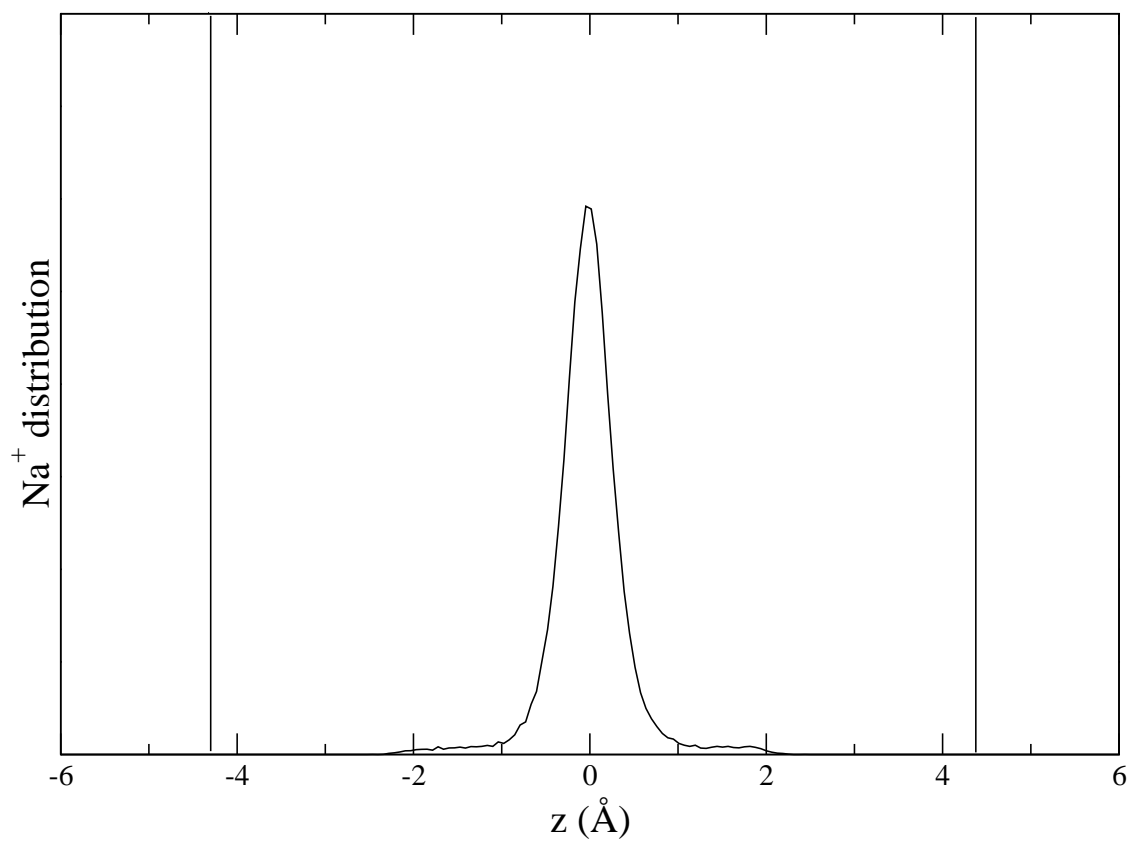


Figure S8:  $\text{Na}^+$  distribution along  $z$  in a bihydrated hectorite, simulated with TIP4P2005/ClayFF force field. This Figure has to be compared to Figure 10 in the main text that shows the case of saponite.

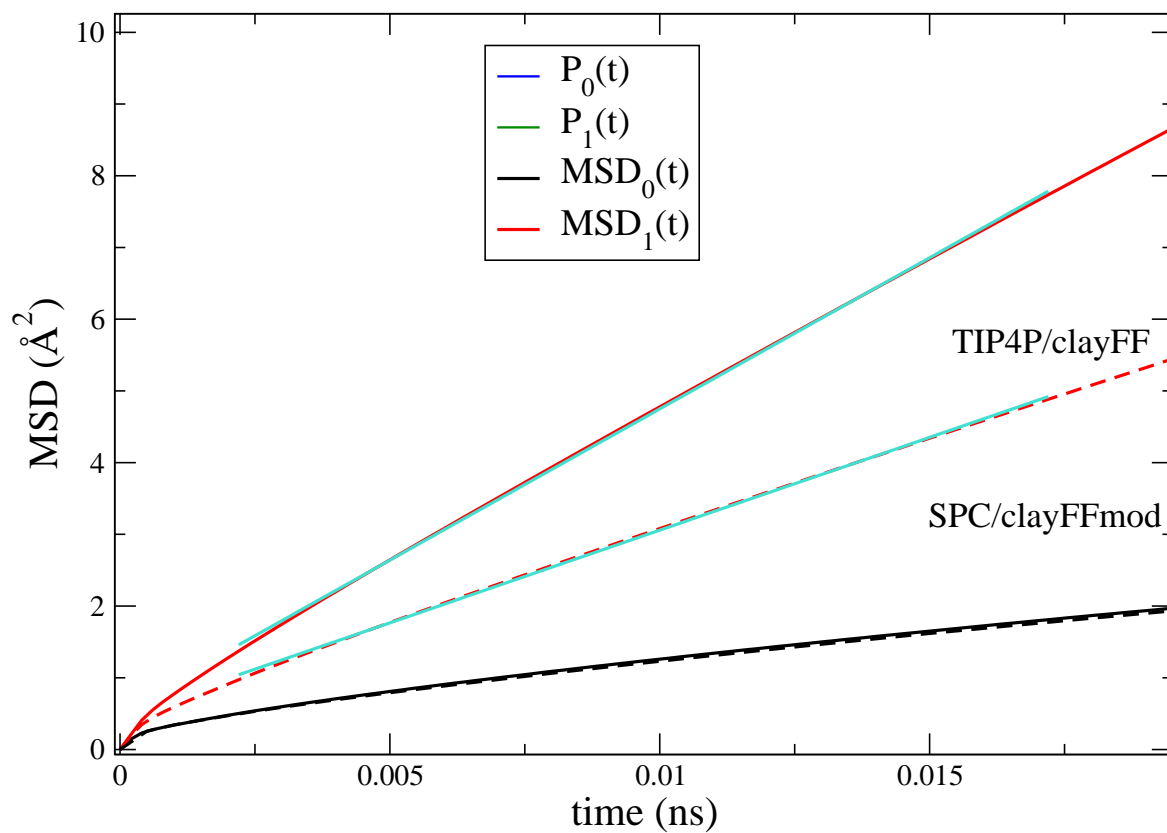


Figure S9: Comparison of the two force fields for the saponite clay at  $T = 300K$ : Solid line: TIP4P2005/clayFF force field, dashed line: SPC/ClayFFmod force field. Zoom of the short times of Figure 11 of the main text, see the legend of Figure 11 for details.

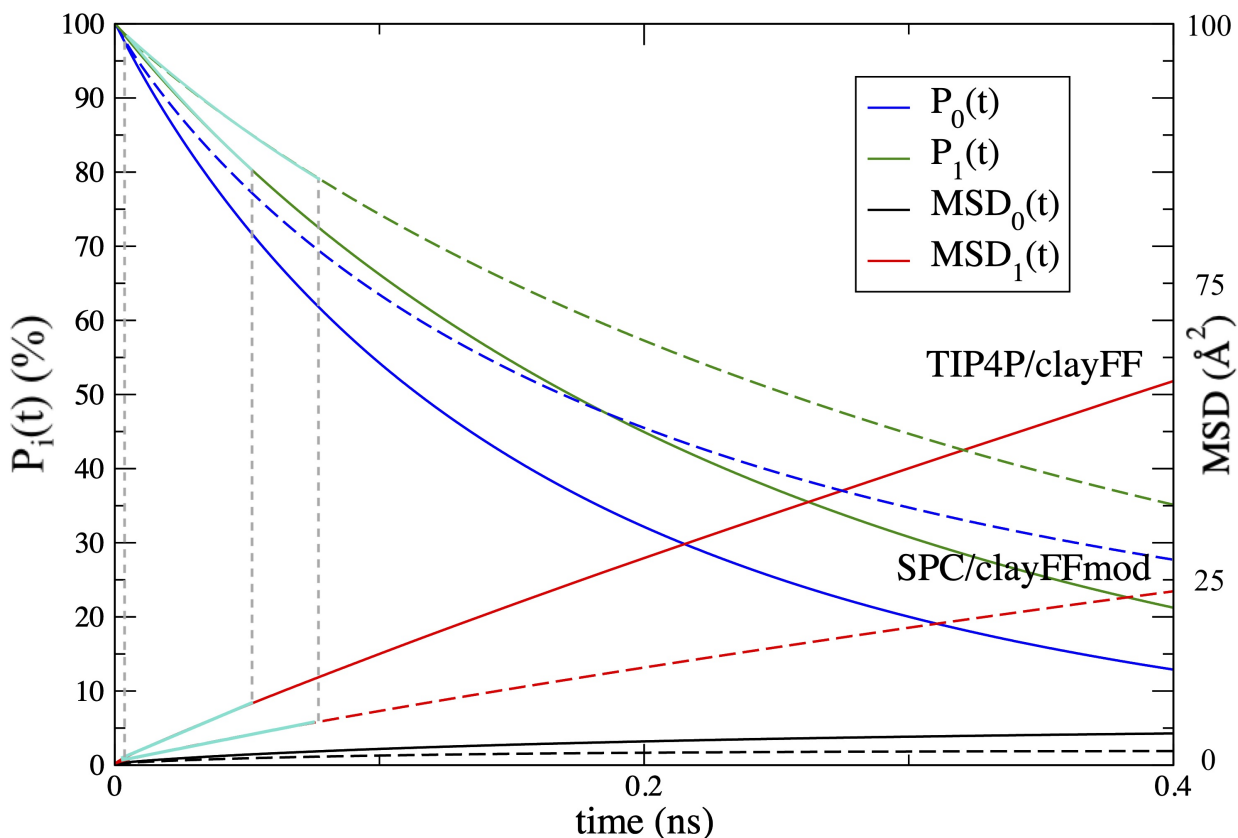


Figure S10: Same plot as the Figure 11 of the main text, here for 250K. Comparison of the two force fields for the saponite clay: Solid lines: TIP4P2005/clayFF force field, dashed lines: SPC/ClayFFmod force field. The subscript 0 (resp. 1) corresponds to water molecules belonging to (resp, not belonging to) the cation hydration spheres (state 0 or state 1). The left scale corresponds to the presence probabilities  $P_i(t)$  (in percents): Blue:  $P_0(t)$ , green:  $P_1(t)$ . The right scale corresponds to the parallel mean-squared displacements  $MSD_i(t) = \frac{\langle x^2 + y^2 \rangle}{2}$  of water molecules in state 0 ( $MSD_0(t)$ , black curves) or state 1 ( $MSD_1(t)$ , red curves). The turquoise highlighted zones correspond to the zone used for the linear regression of  $MSD_1$  to calculate  $D_{\parallel 1}$  (see Table S1 gathering the maximal times used  $\tau_{80\%}$  under which 80% of water in state 1 stayed in state 1).

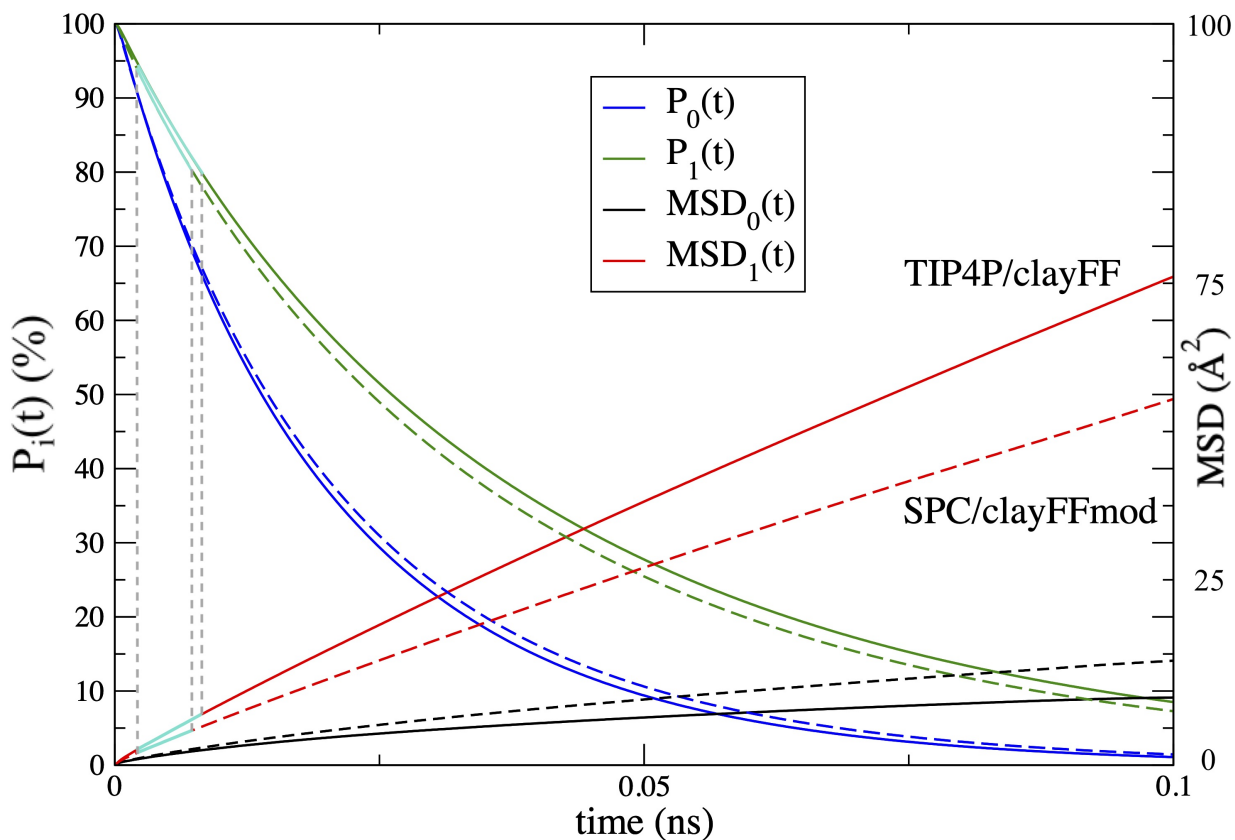


Figure S11: Same plot as the Figure 11 of the main text, here for 350K. Comparison of the two force fields for the saponite clay: Solid lines: TIP4P2005/clayFF force field, dashed lines: SPC/ClayFFmod force field. The subscript 0 (resp. 1) corresponds to water molecules belonging to (resp, not belonging to) the cation hydration spheres (state 0 or state 1). The left scale corresponds to the presence probabilities  $P_i(t)$  (in percents): Blue:  $P_0(t)$ , green:  $P_1(t)$ . The right scale corresponds to the parallel mean-squared displacements  $MSD_i(t) = \frac{\langle x^2 + y^2 \rangle}{2}$  of water molecules in state 0 ( $MSD_0(t)$ , black curves) or state 1 ( $MSD_1(t)$ , red curves). The turquoise highlighted zones correspond to the zone used for the linear regression of  $MSD_1$  to calculate  $D_{\parallel 1}$  (see Table S1 gathering the maximal times used  $\tau_{80\%}$  under which 80% of water in state 1 stayed in state 1).

---

Table S1:  $\tau_{80\%}$  (ps) corresponding to the time after which  $P_1$  has decreased to 80% for the two force fields and the three temperatures studied.

	$\tau_{80\%}$ 255 K	$\tau_{80\%}$ 300 K	$\tau_{80\%}$ 350 K
TIP4P2005/clayFF	54	18.3	8.5
SPC/clayFFmod	75	18	8

## References

- (1) Bée, M. *Quasielastic neutron scattering : principles and applications in solid state chemistry, biology, and materials science*; Adam Hilger, Bristol (UK), 1988; pp 357–362.
- (2) Laage, D.; Hynes, J. T. On the residence time for water in a solute hydration shell: Application to aqueous halide solutions. *J. Phys. Chem. B* **2008**, *112*, 7697–7701.